General Disclaimer

One or more of the Following Statements may affect this Document

- This document has been reproduced from the best copy furnished by the organizational source. It is being released in the interest of making available as much information as possible.

- This document may contain data, which exceeds the sheet parameters. It was furnished in this condition by the organizational source and is the best copy available.

- This document may contain tone-on-tone or color graphs, charts and/or pictures, which have been reproduced in black and white.

- This document is paginated as submitted by the original source.

- Portions of this document are not fully legible due to the historical nature of some of the material. However, it is the best reproduction available from the original submission.

NASA TECHNICAL MEMORANDUM

NASA TM-73809

NASA TM-73809

NOISE OF DEFLECTORS USED FOR FLOW ATTACHMENT WITH STOL-OTW CONFIGURATIONS

by U. von Glahn and D. Groesbeck
Lewis Research Center
Cleveland, Ohio 44135

TECHNICAL PAPER to be presented at the
Ninety-fourth Meeting of the Acoustical Society of America
Miami Beach, Florida, December 13-16, 1977

NOISE OF DEFLECTORS USED FOR FLOW ATTACHMENT WITH STOL-OTW CONFIGURATIONS

by U. von Glahn and D. Groesbeck

National Aeronautics and Space Administration
Lewis Research Center
Cleveland, Ohio 44135

E-9392

ABSTRACT

Future STOL aircraft may utilize engine-over-the-wing (OTW) installations in which the exhaust nozzles are located above and separated from the upper surface of the wing. An external jet-flow deflector can be used with such installations to provide flow attachment to the wing/flap surfaces for lift augmentation. In the present work, the deflector noise in the flyover plane measured with several model-scale nozzle/deflector/wing configurations is examined. The deflector-associated noise is correlated in terms of velocity and geometry parameters. The data also indicate that the effective overall sound pressure level of the deflector-associated noise peaks in the forward quadrant near 40^{o} from the inlet axis.

INTRODUCTION

For future STOL aircraft utilizing engine-over-the-wing (OTW) installations in which the exhaust nozzles are located above and separated physically from the upper surface of the wing, an external jet-flow deflector can be used to attach the flow to the wing/flap surfaces for lift augmentation (fig. 1). Far-field noise measurements were made at model-scale for a number of nozzle/deflector/wing combinations and are reported in reference 1. In reference 2, the jet/surface interaction noise sources were identified and correlated.

STAR Category 07

In the present work, the noise attributed to the deflector configurations used in the work reported in reference 1 is examined. The measured deflector-associated noise, at model-scale, occurred in the frequency range from about 2000 to 20,000 Hz. At these frequencies (2000-20,000 Hz) the wing acts as an acoustic barrier. Consequently, the measured deflector-associated sound pressure levels (SPL) are effective SPL values rather than true SPL values. As a further consequence, the resultant calculated overall sound pressure levels are, therefore, effective values rather than absolute values. The effective deflector noise characteristics are correlated in terms of pertinent jet velocity and configuration geometry parameters.

The acoustic data were obtained with OTW configurations using a conical nozzle with a diameter of 5.2 cm. Flap settings of 20^{o} (takeoff) and 60^{o} (landing) were used with wing chords (flaps retracted) of 33 and 49.5 cm and a span of 61 cm (ref. 1). The nozzle was located at 0.1 chord (flaps retracted) downstream of the wing leading edge and 0.1 chord above the wing surface. The wing sizes are referred to herein as baseline (33 cm chord) and 3/2-baseline (49.5 cm chord). The acoustic data, including spectral plots, were obtained at directivity angles of 60^{o}, 90^{o}, and 120^{o} measured from the inlet axis (ref. 1). All acoustic data were obtained at nominal cold-flow jet velocities of 200 and 259 m/sec.

APPARATUS AND PROCEDURE

Facilities

Aerodynamic facility. - Jet velocity profiles were obtained at the trailing edge of the wing/flap surfaces. These data were obtained at nominal jet exhaust velocities of 200 and 266 m/s as described in reference 1.

Acoustic facility. - The acoustic data were taken at the outdoor facility described in reference 3. In this facility, dry pressurized, ambient temperature air was supplied to the nozzle through a control

valve and valve-noise quieting system. This system consisted of a perforated plate, a four-chamber baffled muffler, and approximately 4.6 m of 10.16-cm diameter piping.

Acoustic data were taken using a horizontal semicircular array of microphones on a 3.05 m radius centered on the nozzle exhaust plane. The 1.27-cm omnidirectional condenser-type microphones used were in a plane level with the nozzle centerline. The microphone angles were 60°, 90°, and 120° measured from the inlet. A mat of 15 cm thick acoustic foam was placed on the ground (asphalt) inside the microphone array to minimize ground reflections. The microphones were 1.52 m above ground level.

Microphone output signals were analyzed by a 1/3-octave-band spectrum analyzer. The analyzer determined sound pressure level (SPL) spectra referenced to 2×10^{-5} N/m^2.

Acoustic measurements were taken over approximately the same range of jet exhaust velocities as those for the aerodynamic measurements; namely, 200 and 259 m/sec (jet Mach numbers of 0.6 and 0.8, respectively). All flow data for the acoustic tests were taken at cold-flow, ambient temperatures near 288 K.

Model Description

Nozzle and deflectors. - The test nozzle consisted of a conical nozzle with a 5.2 cm diameter exit (fig. 2).

The deflector (fig. 2) was held in place by two frames or "tracks" fastened to the nozzle. The deflector could be pivoted to various angles relative to the nozzle centerline. Dimensions of the deflectors used are also given in figure 2. All except one deflector had a span of 7.0 cm (1.35 times the nozzle diameter). This span represents a deflector width that could be stored within the confines of a practical engine nacelle. For one nozzle/wing configuration a deflector with a 14 cm span was also used.

Wings. - The wings (shielding surfaces), installed vertically, are shown schematically in figure 3 together with pertinent dimensions. The surfaces consisted of metal plates secured to wooden ribs. The surfaces

approximated the upper surface contours of the airfoils with the 20^{o} and 60^{o} flap settings used in reference 1. All wings had a span of 61 cm. The nozzle was mounted at the 0.1 chord point of each wing and at 0.1 chord above the wing. The 0.1 chord point is based on the wing chord with flaps retracted. The equivalent flaps-retracted chord sizes for these wings are 33 and 49.5 cm. The wings are referred to by the flap setting of 20^{o} and 60^{o}, and their sizes are referred to as baseline (33 cm chord) and 3/2-baseline (49.5 cm chord).

EXPERIMENTAL RESULTS

General Considerations

The characteristics of deflector-associated noise for an engine over-the-wing (OTW) configuration in which the exhaust nozzle is located above and downstream of the wing leading edge is illustrated in figure 4. Shown in the figure is a curve depicting the nozzle-alone spectrum, nozzle plus wing spectrum (circle symbols), and nozzle/deflector plus wing spectrum (square symbols). The data shown are for a jet Mach number of 0.8, a 40^{o} deflector angle, a deflector length of 4.14 cm, baseline wing, 20^{o} flap setting, and a radiation angle of 60^{o} (forward quadrant). Jet/surface interaction noise sources cause the increased noise evident below about 2000 Hz (greater SPL values, circle and square symbols, compared to the nozzle-alone curve). Without the deflector (unattached flow, circle symbols) jet noise shielding was achieved for frequencies above about 2000 Hz. With the deflector the noise level increased significantly (square symbols) above 2000 Hz, by as much as 17 dB over that for a nozzle alone at 8000 Hz. The SPL data with the deflector, however, are also shielded by the wing because the deflector noise source is located above the wing.

Spectral Considerations

The measured acoustic levels of deflector spectra with a wing are less than those obtained for the nozzle/deflector without a wing (unpublished data), because of the acoustic shielding of the wing. The addition of the wing also shifts the peak frequency, f_p, to a lower value than that for the nozzle/deflector alone configuration (approximately two 1/3-octave bands). The peak frequencies given herein are, therefore, effective values.

If the noise source distribution of the nozzle/deflector plus wing were known, the true deflector noise for the configuration could be synthesized by use of barrier theory. If, as an approximation, the noise source distribution for the nozzle/deflector plus wing is assumed to be the same as that for the nozzle plus wing, an acoustic shielding correction can be added to the measured deflector noise spectra based on the nozzle plus wing shielding data. The addition at each frequency of a ΔSPL to account for the acoustic shielding determined from the nozzle/wing tests to the measured SPL values for the deflector SPL values should yield an approximate deflector noise spectra independent of the acoustic shielding of the wing. This procedure was followed with the result that the synthesized deflector spectra had the same shape and peak frequency as the measured nozzle/deflector spectra (unpublished data) but was about 2 dB lower in absolute magnitude. This difference is attributed to the fact that the noise source distributions with and without the deflector are not the same.

In the present report, the deflector noise data are correlated in terms of an effective spectral shape and peak frequency which include the acoustic shielding benefits associated with each wing size used in the tests. The resultant correlation is therefore strictly applicable only to the nozzle/deflector/wing configurations discussed herein; however, on the basis of limited unpublished data, noise estimates for other configurations similar to those tested appear to be permissible.

Deflector spectra. - The spectral shape of the deflector-associated noise was obtained for each configuration by fairing a curve through the

data such as that shown in figure 4 for the square symbols. OASPL values were calculated for each curve. Data were selected in which there was sufficient SPL separation between the nozzle/wing data with and without the deflector so that the deflector-associated noise levels were substantially independent of, or required little correction (<1 dB) for the shielded jet noise levels (circle symbols). The tone that appeared in much of the data at 6300-8000 Hz is believed to be associated with the small-scale aspects of the configuration and is assumed not to occur at full scale. Consequently, the tone was disregarded in establishing each deflector noise spectral shape. The effective deflector noise spectral shape that resulted is given in figure 5 in terms of the reduction in sound pressure level with respect to that at the peak frequency, $(SPL-SPL_p)$ as a function of 1/3-octave band frequency intervals.

Frequency. - A modified Strouhal number at the frequency of the peak SPL for the deflector associated noise was obtained for each configuration and is given by the following relationship:

$$\frac{f_p D}{U_j}\left[\frac{\ell}{D}\right]^{0.167}\left[1+\frac{L}{D}\right]^{0.0833} = 1.25 \qquad (1)$$

For the L/D values herein, equation (1) can be simplied to:

$$\frac{f_p D}{U_j}\left[\frac{\ell}{D}\right]^{0.167} = 1.0 \qquad (2)$$

Thus, the peak frequency, f_p, for the present deflector configurations is independent of wing size, deflector angle and deflector width.

Deflector Geometry Effects

The purpose of the external deflector in STOL-OTW applications is to redirect and to attach the jet exhaust efflux to the wing, thereby providing lift augmentation during landing and takeoff. In order to assess

the flow attachment potentials several deflector sizes and deflector settings were studied (ref. 1). Because the deflector immersions in the jet flow differed, each deflector size at each angle setting provided its own noise signature. The following sections summarize the deflector geometry effects on the deflector associated noise signature. The discussion centers on the spectra at frequencies greater than 2000 Hz and disregards the tones frequently shown at 6300-8000 Hz.

Radiation angle. - The effect of radiation angle on the deflector noise is shown in figure 6 for a representative configuration. The configuration selected is that described for figure 4 and the data shown are for $\theta = 60^{o}$, 90^{o}, and 120^{o}. It is apparent that, for the case shown, the deflector associated SPL levels decrease with increasing radiation angles.

Deflector setting. - A typical spectral variation with deflector angle (β) is shown in figure 7. The data shown are for the baseline wing, $\theta = 60^{o}$, 20^{o} flap setting, $M_j = 0.8$ and a deflector length of 4.14 cm. Also shown for comparison are the nozzle/wing and nozzle alone spectra. It is evident that the SPL values increase with an increase in deflector angle.

Deflector size. - Representative spectra illustrating the effect of deflector length (constant width, w = 7 cm) on the noise level are shown in figure 8. The data shown are for a 3/2-baseline wing, 60^{o} radiation angle, 60^{o} flap setting, deflector angle, 40^{o} and M_j, 0.8. In general, the spectral level increases and the peak SPL shifts to a lower frequency with an increase in deflector length.

Deflector width. - A single test configuration was used to assess the effect of increasing the width of the deflector on the spectral shape and level. The results are shown in figure 9 in which spectral data for deflector widths of 7.0 and 14 cm are compared. The data were obtained with the 3/2-baseline wing, 60^{o} radiation angle, 60^{o} flap setting, deflector angle, 40^{o}, deflector length, 7.9 cm, and M_j, 0.8. The increase in deflector width caused a broadband increase in noise level.

CORRELATION

The systematic varying of the configuration geometry (wing size and deflector size and angle) for jet exhaust Mach numbers of 0.6 and 0.8 provide the input for an empirical correlation of the measured acoustic data. The initial data analysis indicated that the effective deflector OASPL varied approximately with the 6-power of the jet exhaust velocity and was a function of the deflector angle as shown in figure 10. The data shown are for the baseline wing, 20^{o} flap setting, 60^{o} radiation angle and a deflector length of 4.14 cm. (The 60^{o} radiation angle was selected for figure 10 in order to provide the largest OASPL separation between nozzle/wing acoustic data with and without a deflector.) The data trend shown in figure 10 is representative of all configurations tested; with only the level of the noise differing for each nozzle/deflector/wing configuration tested. It appears that the data should follow a curved line rather than a straight line since at $\beta = 0^{o}$, the deflector would still be a noise source.

In addition to the variables included in figure 10, the effective deflector noise level is a function of the wing size, deflector length, and deflector width. The inclusion of the first two of these factors in the data correlation is shown in figure 11. The data shown are for a 60^{o} radiation angle. Note that the data points shown are for OASPL levels calculated from fairing the effective spectral shape (fig. 5) through the measured SPL data. The data scatter shown in figure 11 is primarily due to this fairing. For the range of geometries included, the effect of the deflector length on the noise level is expressed by the term $-10 \log \ell/D$ in the ordinate of figure 11. The wing size affects the deflector noise because the amount of "barrier" shielding varies with wing size. The term $+10 \log (1 + L/D)$ approximates this effect of wing size on the effective deflector noise. The form of this term preserves continuity of the correlation (i.e., the noise level of the deflector does not go to zero) when the wing is removed.

An increase in the deflector width, based on the single configuration tested, caused the effective deflector noise to increase in a manner that

was proportional to the increase in width. In order to include the deflector width as a variable, the ordinate of figure 11 can be amended by the inclusion of a term given by -10 log w/D. For practical applications, the term w/D is generally limited to a range of 1.2 to 1.5. Thus, the effect of deflector width on the effective deflector noise (~1 dB) can be neglected for practical applications.

Data correlations similar to that in figure 11 are shown in figure 12 for radiation angles of 90^{o} and 120^{o}. Fewer data points are available for these radiation angles than for the 60^{o} radiation angle because of the difficulty in obtaining deflector SPL values that were uncontaminated by, or could be corrected for, jet exhaust noise. The curves shown in figure 12 are the same as those shown in figure 11 but reduced in level with increasing radiation angle.

The reduction of the effective deflector OASPL with increasing radiation angle is shown in figure 13 for radiation angles of 60^{o}, 90^{o}, and 120^{o}. The data trend shown is for a 40^{o} deflector angle, but is representative of other deflector angles. Unpublished data (dashed curve, fig. 13) taken over a greater range of radiation angles shows that the maximum effective deflector OASPL occurs at an approximate radiation angle of 40^{o}. The radiation pattern shown in figure 13 is strictly applicable only to the wing sizes and nozzle/deflector/wing configurations used herein. On the basis of unpublished nozzle/deflector OASPL data, the use of much smaller wing sizes than those herein, should shift the peak OASPL from 40^{o} toward higher radiation angles (approaching θ-values of 80^{o}-90^{o}).

CONCLUDING REMARKS

The use of external jet-flow deflectors to achieve flow attachment and thereby augmented lift for STOL-OTW aircraft can cause a significant noise increase in the forward quadrant. This increase is particularly evident when the jet exhaust nozzle is mounted some distance above the wing in an effort to optimize the lift/drag for cruise. In the present configurations, the nozzle exhaust plane was at 0.1 chord (flaps re-

tracted). However, unpublished acoustic data taken with the same nozzle, deflectors, and wings but with the nozzle exhaust plane located at 0.21 chord showed little difference in the effective deflector noise characteristics.

Although the deflector correlation presented herein is strictly applicable to the nozzle/deflector/wing configurations tested, sufficient information (some unpublished) exists to suggest that it can be extended to other practical types of OTW configurations using above-wing mounted nozzles with external deflectors.

NOMENCLATURE

A	nozzle exhaust area
C	wing chord (flaps retracted); see figure 3
D	nozzle exhaust diameter
f_p	peak 1/3-octave band frequency for a given noise source
L_s	shielding surface length
L_f	wing length upstream of nozzle exhaust plane
L	projected shielding surface length
ℓ	effective deflector length
M_j	jet exhaust Mach number
OASPL	overall sound pressure level, dB re 2×10^{-5} N/m^2
SPL	sound pressure level, dB re 2×10^{-5} N/m^2
SPL_P	peak sound pressure level, dB re 2×10^{-5} N/m^2
U_j	jet exhaust velocity
w	spanwise width of deflector
α	flap setting (angle)
β	deflector angle
θ	acoustic radiation angle measured from nozzle inlet

REFERENCES

1. U. von Glahn and D. Groesbeck, "Effect of External Jet-Flow Deflector Geometry on OTW Aero-Acoustic Characteristics," NASA TM X-73460, 1976.

2. U. von Glahn and D. Groesbeck, "Interim Noise Correlation for Some OTW Configurations Using External Jet-Flow Deflectors," NASA TM 73746, 1977.

3. M. Reshotko and R. Friedman, "Acoustic Investigation of the Engine-Over-the-Wing Concept Using a D-Shaped Nozzle," AIAA Paper 73-1030, Oct. 1973.

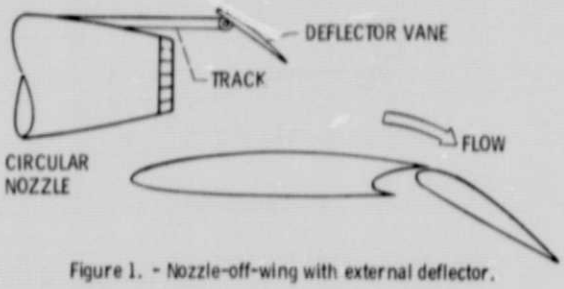

Figure 1. - Nozzle-off-wing with external deflector.

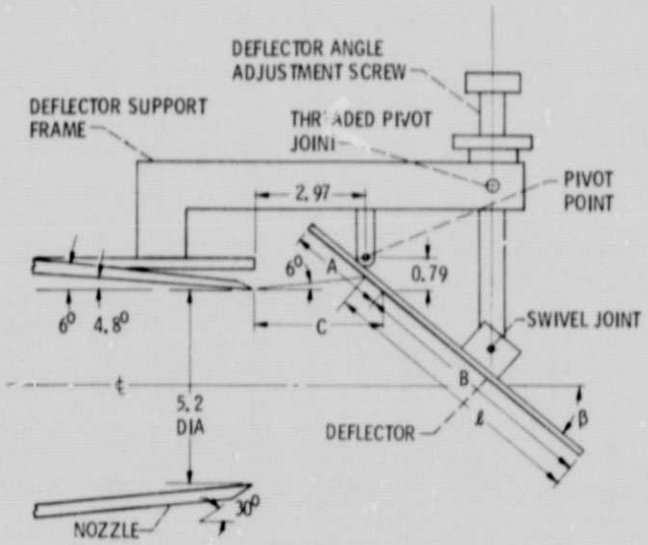

ℓ	A	B	C	β
1.95	2.41	1.04	3.86	20°
	2.24	1.21	3.63	25°
	2.13	1.32	3.51	30°
	2.03	1.42	3.25	40°
4.14	2.51	3.18	3.91	20°
	2.29	3.40	3.66	25°
	2.18	3.51	3.51	30°
	2.06	3.63	3.25	40°
7.90	2.54	6.91	4.01	20°
	2.31	7.14	3.66	25°
	2.11	7.34	3.40	30°
	2.03	7.42	3.18	40°

Figure 2. - Schematic sketches of nozzle and flow deflectors. (All dimensions in centimeters.)

E-9392

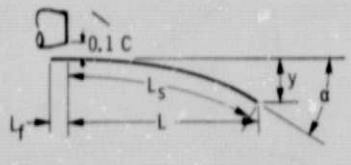

WING DIMENSIONS

FLAP ANGLE, α, DEG	CONFIGURATION	y, CM	L_f, CM	L, CM	L_s, CM
20	BASELINE	6.6	3.3	37.4	39.0
	3/2-BASELINE	10.2	5.0	56.0	58.4
60	BASELINE	14.3	3.3	34.1	42.3
	3/2-BASELINE	21.5	5.0	50.9	62.8

Figure 3. - Wing dimensions.

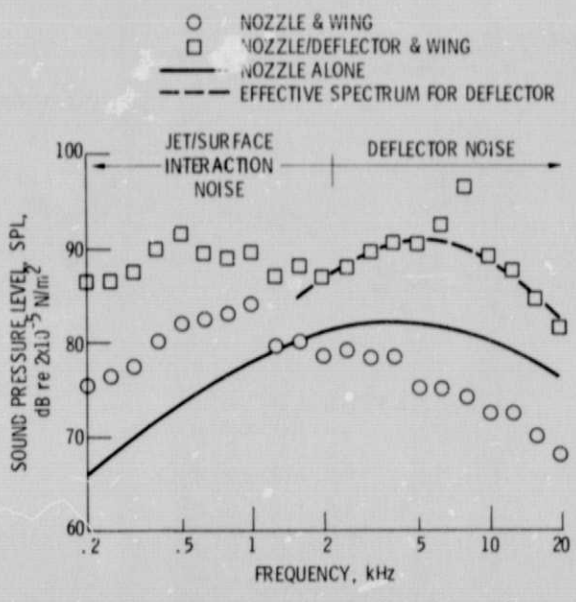

Figure 4. - Comparison of spectra for various configurations. Baseline wing; 20^0 flap setting; 40^0 deflector setting; deflector length, 4.14 cm; M_j, 0.8; radiation angle, θ, 60^0.

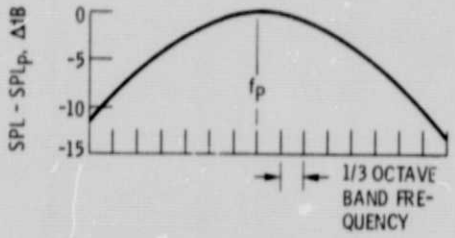

Figure 5. - Effective deflector noise source spectral shape.

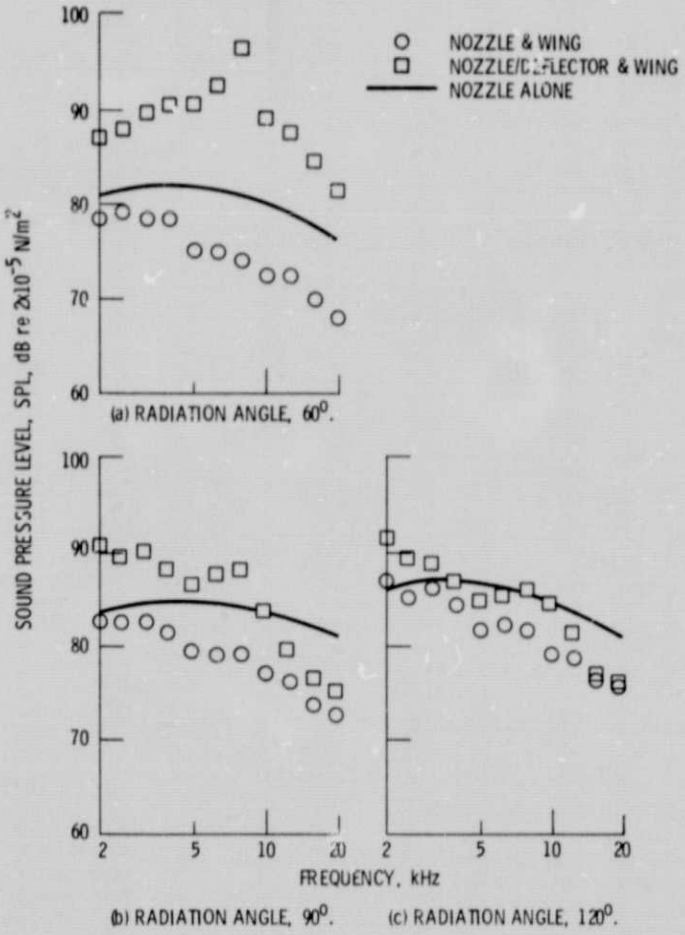

(a) RADIATION ANGLE, 60°.

(b) RADIATION ANGLE, 90°. (c) RADIATION ANGLE, 120°.

Figure 6. - Typical variation of deflector spectra with radiation angle, θ. Baseline wing; 20° flap setting; 40° deflector setting; deflector length, 4.14 cm; M_j, 0.8.

E-9392

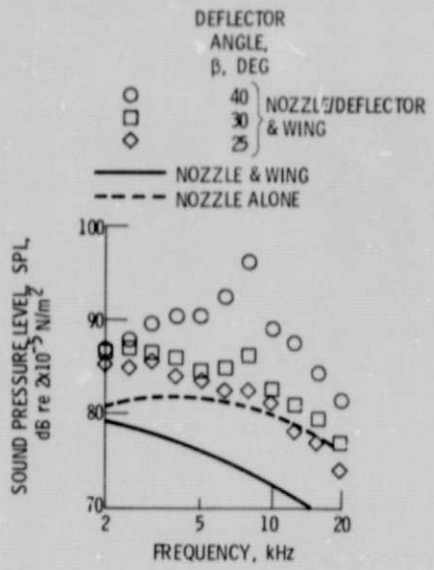

Figure 7. - Variation of deflector spectra with deflector angle. Baseline wing; 20^0 flap setting; deflector length, 4.14 cm; M_j, 0.8; 60^0 radiation angle.

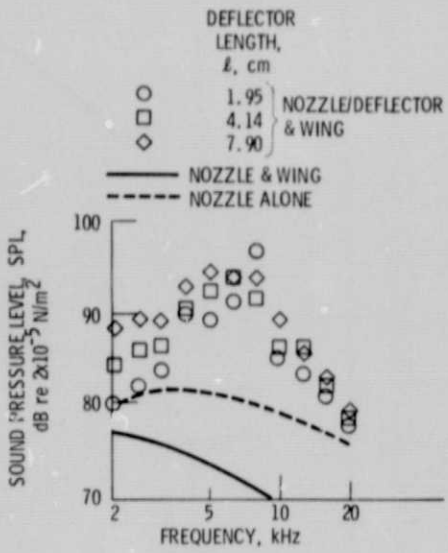

Figure 8. - Variation of deflector spectra with deflector length, ℓ. 3/2-baseline wing; 60^0 flap setting; 40^0 deflector setting; M_j, 0.8; 60^0 radiation angle.

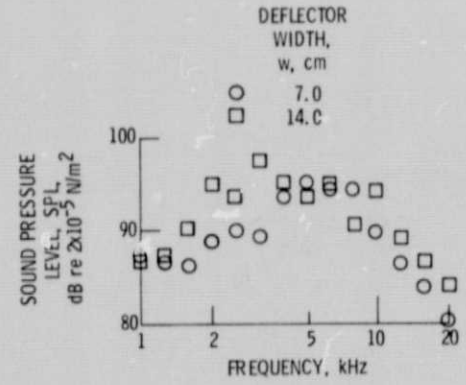

Figure 9. - Effect of deflector width, w, on deflector spectra. 3/2-baseline wing; 60^0 flap setting; 40^0 deflector setting; deflector length, 7.9 cm; M_j, 0.8; 60^0 radiation angle.

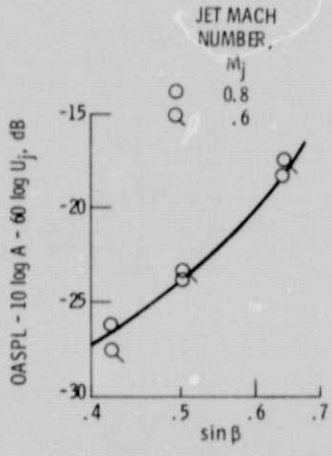

Figure 10. - Representative variation of effective deflector OASPL with deflector angle, β. Baseline wing; 20^0 flap setting, 60^0 radiation angle; deflector length, 4.14 cm.

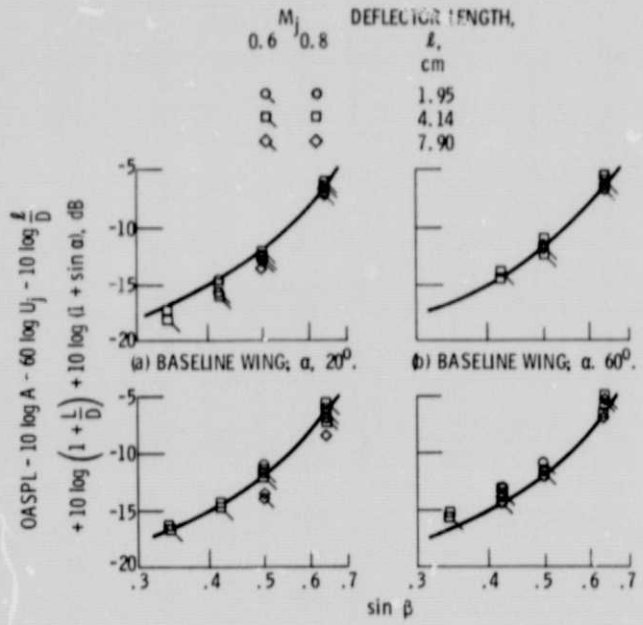

Figure 11. - Correlation of effective deflector OASPL. 60° radiation angle.

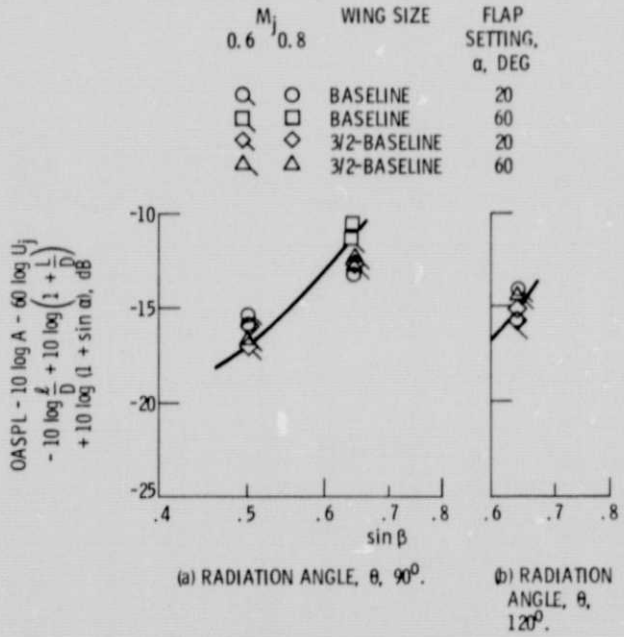

Figure 12. - Correlation of effective deflector OASPL. Radiation angles, 90° and 120°; deflector length, 4.14 cm.

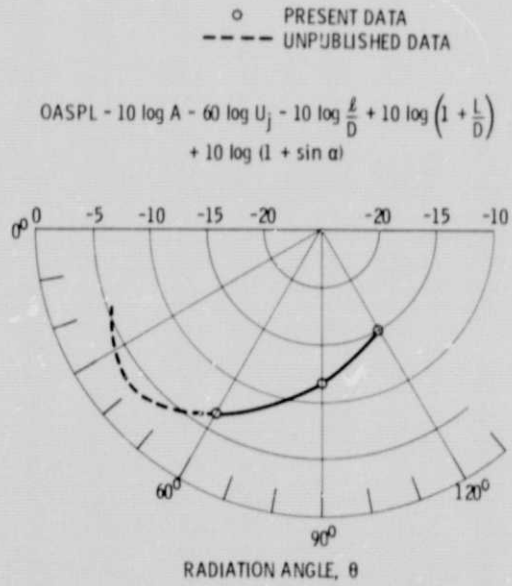

Figure 13. - Typical radiation pattern for effective deflector correlation parameter. 40° deflector angle.